Supplementary Information

Group	Weight of tumor (mg)			
	LMD-PSMA	LMD	PC3-PIP	PC3-Flu
J591	544 ± 229	607 ± 314	459 ± 258	820 ± 222
J591-PEG10k	570 ± 192	471 ± 123	601 ± 107	725 ± 152
J591-PEG30k	512 ± 269	334 ± 182	536 ± 295	630 ± 282

Table S1: Weight of the tumors. After the last imaging time point animals were sacrificed and tumors excised. The excised tumors were weighed using a scientific balance. The table represents the average weight of the tumors (N=5) along with standard deviations.

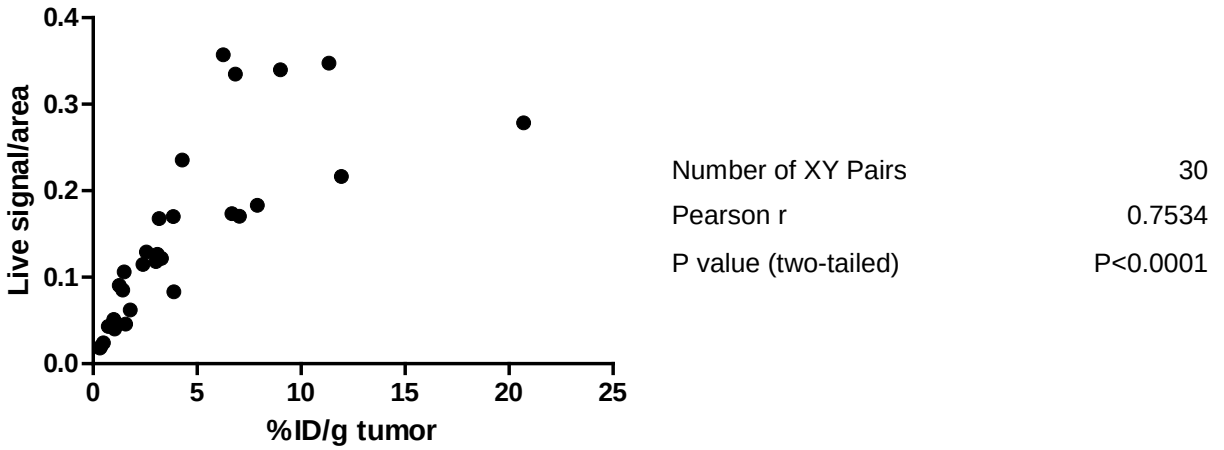

Figure S1: Correlation of *in vivo* NIR imaging and *ex vivo* biodistribution analysis. Animals bearing bi-lateral LMD/LMD-PSMA tumors were intravenously injected with J591-IR800. At multiple time points (24-120 h) live animals (N=3 per time point) were first imaged by LICOR-PEARL imaging. Immediately after the live imaging, animals were sacrificed and the tumors were excised, weighed and lysed as described in (1). The IR800 fluorescence signal from tumor lysates was measured by LICOR odyssey fluorescent scanning and relative quantity determined by reference to a serially diluted J591-IR800 standard. The resulting data was converted to %ID/g and compared with live signal/area. The correlation of live signal/area (Y-axis) versus IR800 signal %ID/g tumor (X-axis) demonstrates a linear and significant correlation, supporting the use of live animal imaging for real-time pharmacokinetic analysis of J591-conjugates. The resulting Pearson r correlation and p values are indicated.

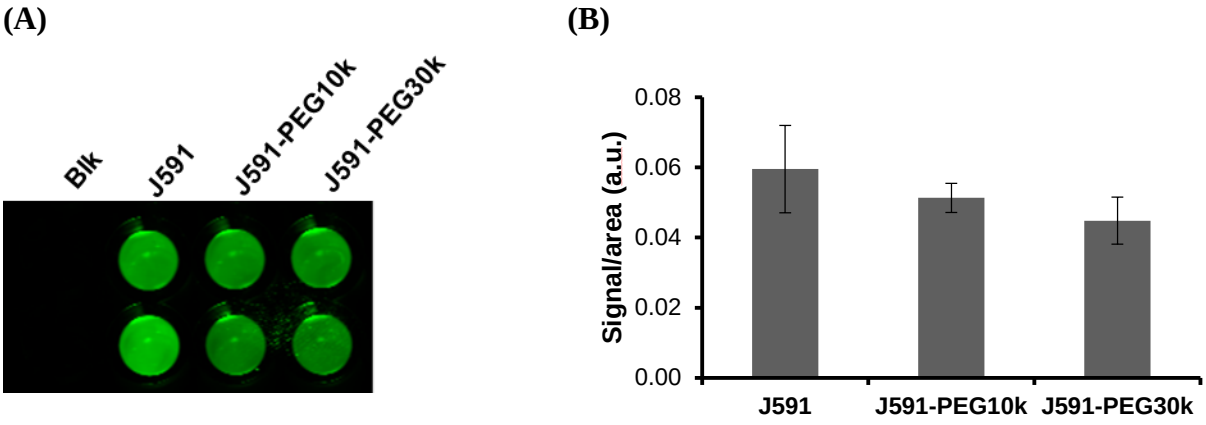

Figure S2: Evaluation of injected J591-conjugates. (A) Aliquots of J591-conjugate preparations used for systemic injection in LMD tumor models (Figure 4) were diluted 1:100 with PBS and transferred to a 96 well plate (in duplicate). IR800 fluorescence imaging by LICOR-odyssey support that comparable IR800 levels of each J591 conjugates were administered for each experiment. (B) Comparative analysis of J591-conjugate uptake in muscle (fluorescence intensity per area) 24 h post-injection (N=5 per group) from LMD tumor model experiments (Figure 4) support comparable injection levels across conjugates and experiments. Error bars represent standard deviation.

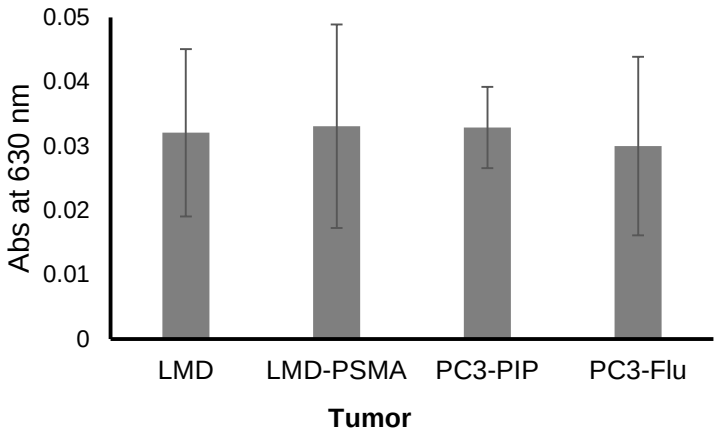

Figure S3: Assessment of tumor vascular permeability. Tumor vascular permeability was measured as described by Kunjachan S *et al* (2). Briefly, tumor bearing mice (N=3 per group) were systemically injected with 200 µL of 1mg/mL Evans Blue dye (Sigma-Aldrich, St. Louis, MO). 48 h post injection tumors were removed and Evans blue was extracted using formamide (0.01 mL/mg of tumor) and quantified by Absorbance at 630 nm. There were no significant differences observed in the average absorbance between the four tumor groups. Error bars represent standard deviation.

(A)

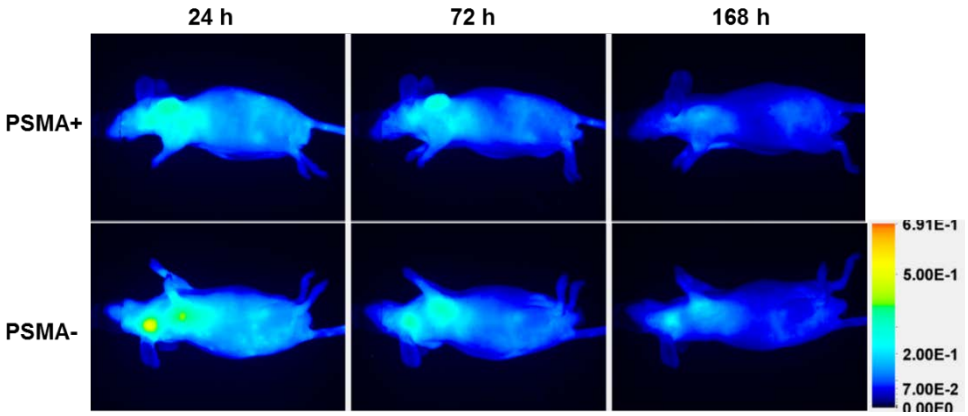

(B)

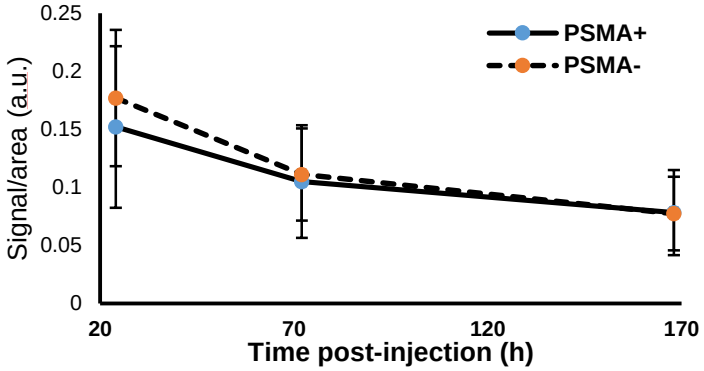

Figure S4: Passive dye uptake in PSMA-positive and PSMA-negative tumors. (A) Mice bearing contra-lateral isogenic PSMA+/- (LMD-PSMA/LMD) tumors were injected with the non-specific PEG-IRdye800 (N=4), a contrast agent designed to evaluate EPR targeting. The image shows a representative mouse imaged with LICOR-PEARL imager 24, 72 and 168 h post-injection. The dye accumulated similarly in both PSMA positive and negative tumors at all time-points. (B) Average NIR signal per area over time (N=4) as quantified by NIR imaging. Error bars represent standard deviation. No significant differences were detected between PSMA positive and PSMA negative tumors.

(A)

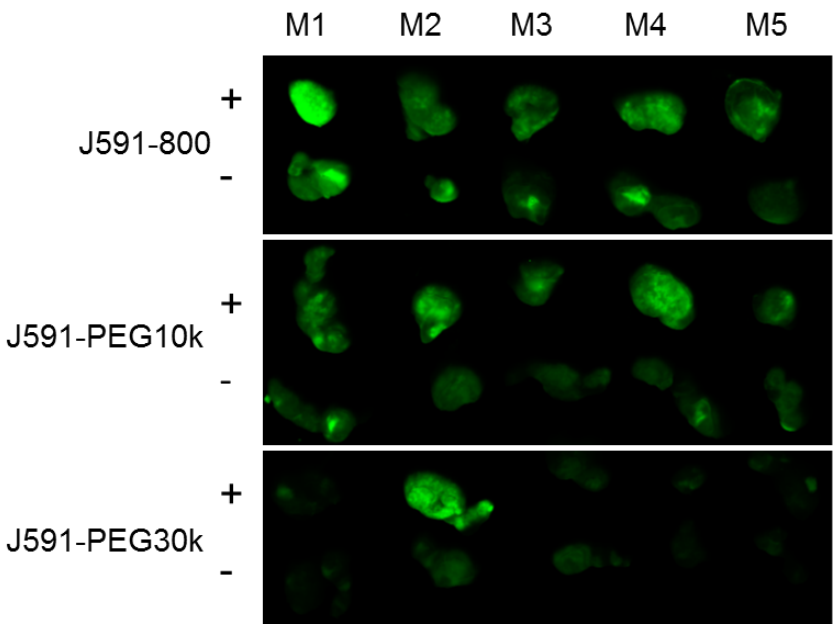

(B)

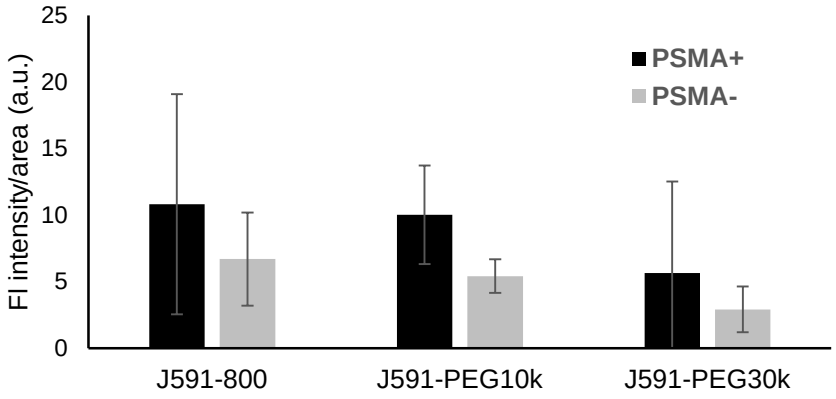

Figure S5: *Ex vivo* tumor image analysis of LMD/PSMA xenograft model (A) After the last imaging time-point (120 h) animals were sacrificed and tumors were harvested. Whole excised tumors were imaged by LICOR-odyssey scanner at equal exposure. The image shows the tumors for all 5 mice injected with J591-IR800k, J591-PEG10k or J591-PEG30k. (B) Average quantitative fluorescence intensity of tumors per area of tumor (N=5). Error bars represent standard deviation.

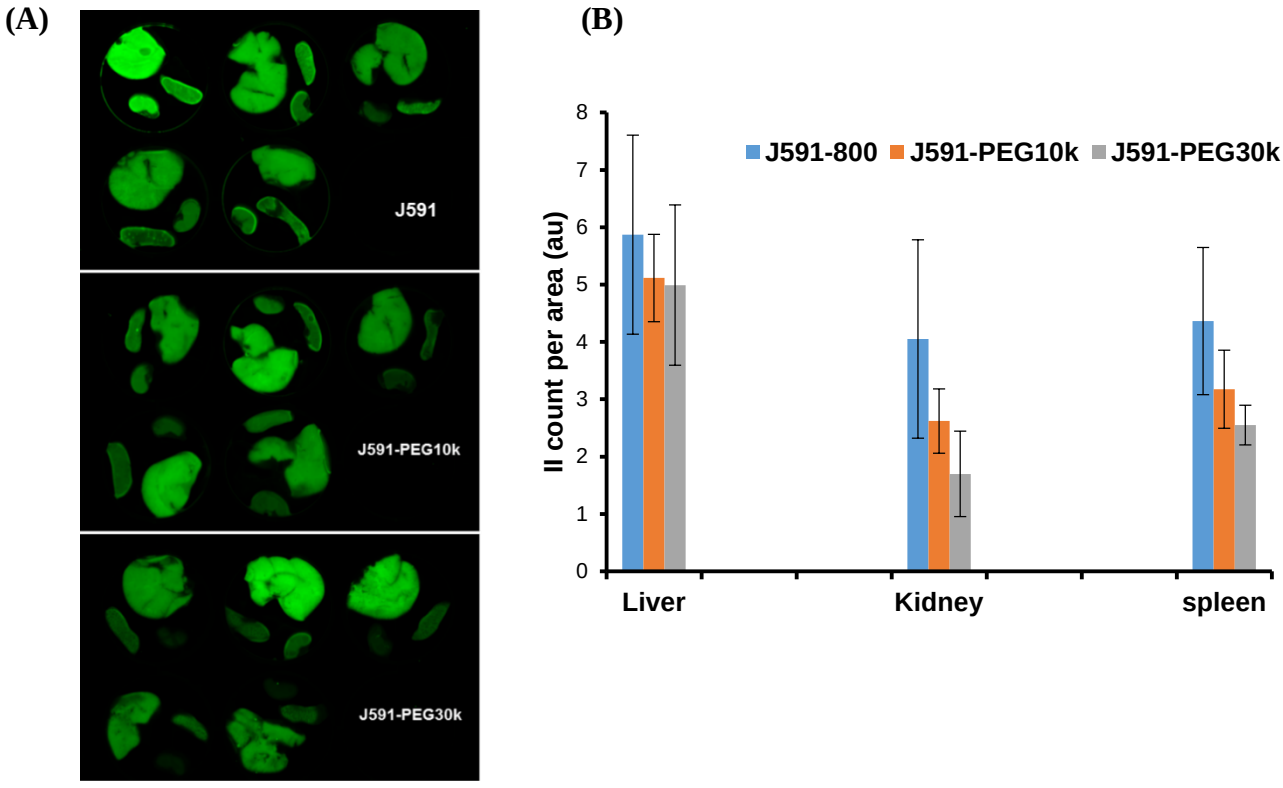

Figure S6: *Ex vivo* biodistribution analysis of J591-conjugates in LMD tumor model (A) After the last imaging time-point (120 h) animals were sacrificed and select organs harvested. The harvested organs (liver, spleen and kidney) were imaged *ex vivo by* LICOR-odyssey scanner at equal exposure. The image shows the organs for all 5 mice injected with J591-IR800, J591-PEG10k or J591-PEG30k. (B) Average quantitative fluorescence intensity of organs per area (N=5). Error bars represent standard deviation.

(A)

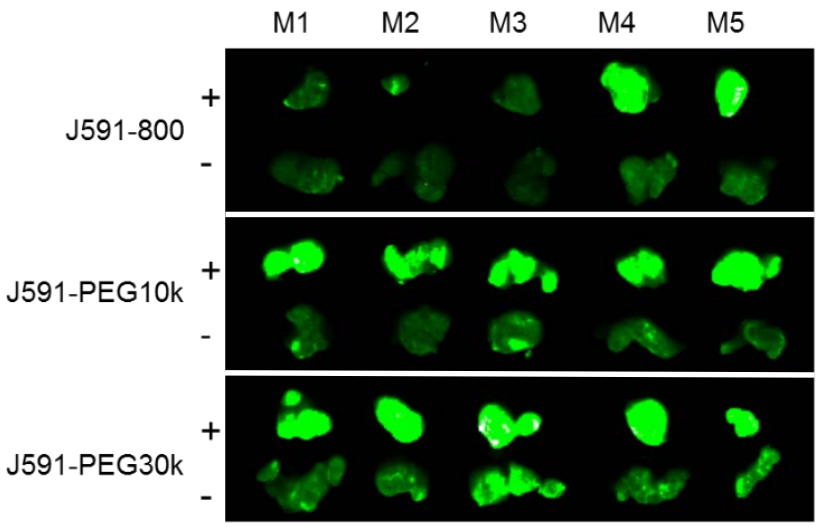

(B)

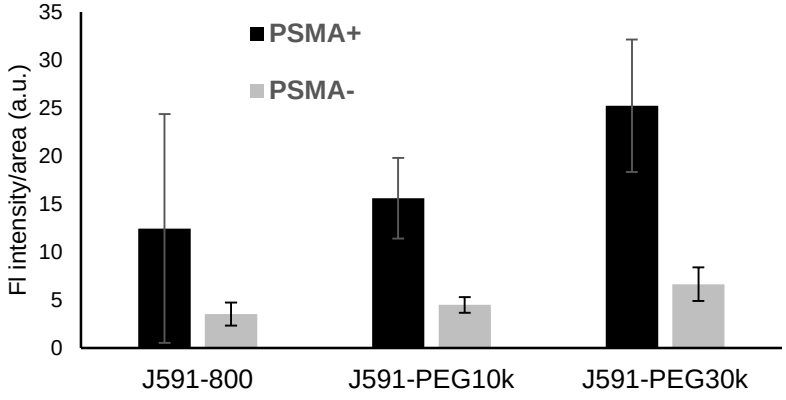

Figure S7: *Ex vivo* tumor image analysis of PC3/PSMA xenograft model (A) After the last imaging time-point (120 h) animals were sacrificed and tumors were harvested. Whole excised tumors were imaged by LICOR-odyssey scanner at equal exposure. The image shows the tumors for all 5 mice injected with J591-IR800k, J591-PEG10k or J591-PEG30k. (B) Average quantitative fluorescence intensity of tumors per area of tumor (N=5). Error bars represent standard deviation.

(A)

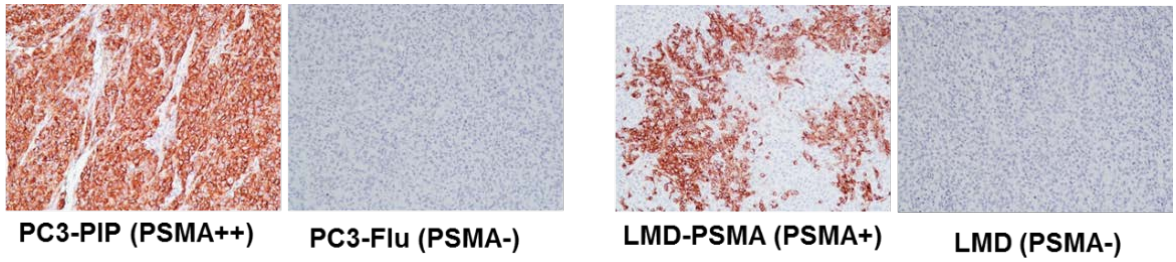

(B)

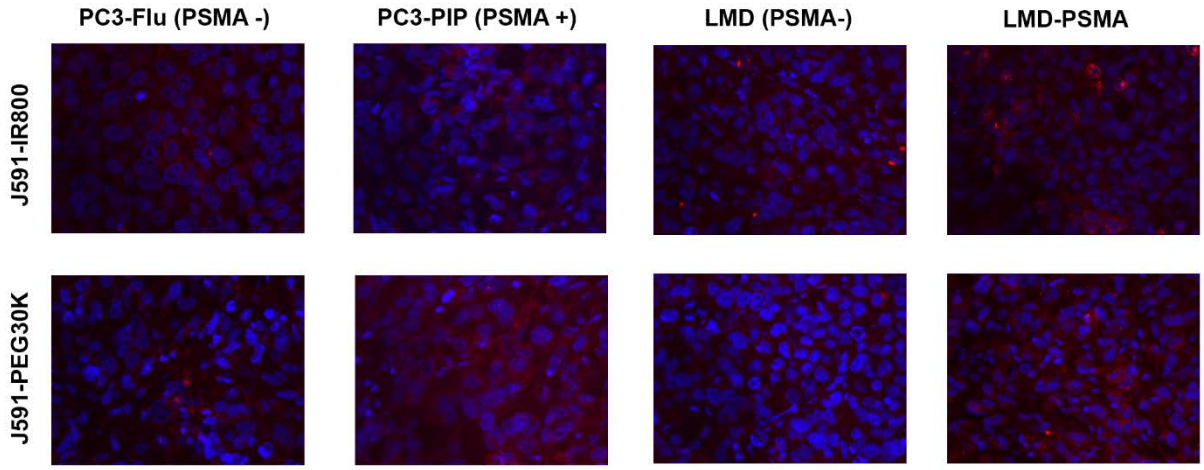

Figure S8: PSMA expression and J591 conjugate distribution. PSMA expression and J591-IR800 and J591-PEG30k tumor uptake in LMD ± PSMA and PC3 ± PSMA isogenic tumor models 24 h post-injection. Whole tumors were isolated, fixed and analyzed by IHC and immunofluorescent microscopy. (A) Anti-PSMA immunohistochemistry performed on dissected tumors sections. 10X magnification. Results confirm PSMA-specific expression and support higher PSMA expression by the PC3 model. (B) Immunofluorescent microscopy of J591 conjugate intratumoral distribution in PSMA-negative and PSMA-positive PC3 and LMD tumors by anti-human IgG fluorescent microscopy. 40X magnification. Red, HuJ591; Blue, DAPI.

References:

1. Oliveira S, Cohen R, Walsum MS, van Dongen GA, Elias SG, van Diest PJ, et al. A novel method to quantify IRDye800CW fluorescent antibody probes ex vivo in tissue distribution studies. EJNMMI research 2012;2(1):50.
2. Kunjachan S, Pola R, Gremse F, Theek B, Ehling J, Moeckel D, et al. Passive versus active tumor targeting using RGD- and NGR-modified polymeric nanomedicines. Nano letters 2014;14(2):972-81.